Integrating AlInN interlayers into InGaN/GaN multiple quantum wells for enhanced green emission

Wei Sun, Syed Ahmed Al Muyeed, Renbo Song, Jonathan J. Wierer, and Nelson Tansu

Citation: Appl. Phys. Lett. **112**, 201106 (2018); doi: 10.1063/1.5028257
View online: https://doi.org/10.1063/1.5028257
View Table of Contents: http://aip.scitation.org/toc/apl/112/20
Published by the American Institute of Physics

Integrating AlInN interlayers into InGaN/GaN multiple quantum wells for enhanced green emission

Wei Sun,[a)] Syed Ahmed Al Muyeed, Renbo Song, Jonathan J. Wierer, Jr., and Nelson Tansu[a)]

Center for Photonics and Nanoelectronics, Department of Electrical and Computer Engineering, Lehigh University, Bethlehem, Pennsylvania 18015, USA

(Received 8 March 2018; accepted 8 May 2018; published online 16 May 2018)

Significant enhancement in green emission by integrating a thin AlInN barrier layer, or interlayer (IL), in an InGaN/GaN multiple quantum well (MQW) is demonstrated. The MQWs investigated here contains 5 periods of an InGaN QW, a 1 nm thick AlInN IL, and a 10 nm thick GaN barrier grown by metalorganic chemical vapor deposition. To accommodate the optimum low-pressure (20 Torr) growth of the AlInN layer a growth flow sequence with changing pressure is devised. The AlInN IL MQWs are compared to InGaN/AlGaN/GaN MQWs (AlGaN IL MQWs) and conventional InGaN/GaN MQWs. The AlInN IL MQWs provide benefits that are similar to AlGaN ILs, by aiding in the formation of abrupt heterointerfaces as indicated by X-ray diffraction omega-2theta (ω-2θ) scans, and also efficiency improvements due to high temperature annealing schedules during barrier growth. Room temperature photoluminescence of the MQW with AlInN ILs shows similar performance to MQWs with AlGaN ILs, and ~4–7 times larger radiative efficiency (pump intensity dependent) at green wavelengths than conventional InGaN/GaN MQWs. This study shows the InGaN-based MQWs with AlInN ILs are capable of achieving superior performance to conventional InGaN MQWs emitting at green wavelengths. *Published by AIP Publishing.*
https://doi.org/10.1063/1.5028257

InGaN-based multiple quantum wells (MQWs) have achieved tremendous success as high efficiency active regions in blue light-emitting diodes (LEDs) and laser diodes (LDs).[1–9] These blue LEDs and LDs are integrated with phosphors to create the most efficient white sources ever created.[6–9] However, to achieve an even higher efficiency white light source and enable smart functionalities such as color temperature tuning,[6] white sources created from direct emitters (blue, green, and red) are required.[7] Therefore, creating InGaN-based MQWs emitting at green to red wavelengths becomes essential. Longer wavelength InGaN-based MQWs require a significant increase in In-content within the QWs, which in turn results in low efficiency active regions compared to the blue.[7,8] The efficiency reduction in InGaN-based MQWs emitting in the green-red is attributed to multiple reasons including phase separation in high In-content InGaN;[10,11] defects induced by strong lattice mismatch strain;[12–14] low growth temperatures in order to incorporate higher In-concentration that introduces impurities and defects;[15,16] and charge separation caused by strong, built-in polarization fields.[17–19]

Several solutions have been proposed to enhance the efficiency of green- and red-emitting InGaN-based MQWs, including the use of large overlap QW active regions,[18–21] non- and semi-polar QWs,[22,23] ternary substrates,[24,25] and AlGaN interlayers (ILs) in InGaN MQW.[26–31] Specifically, AlGaN tensile barriers or ILs provide various benefits for higher efficiency green-red LEDs.[26–31] The AlGaN IL behaves as a "cap" layer that suppresses out-diffusion of indium from the InGaN QW and produces a more abrupt heterointerfaces.[26,27] It also enables strain compensation and promotes pseudomorphic growth with suppressed defect formation.[29–31] Finally, the structure also enables annealing of InGaN QW during GaN barrier growth at higher temperatures that improves efficiencies.[27]

AlInN is another potential IL choice for InGaN-based MQWs with potential advantages over AlGaN ILs. First, the strain state of the AlInN can be tuned with respect to GaN by changing In-content, from heavily tensile strained, to nearly lattice-matched, to compressively strained.[32] Therefore, an AlInN IL enables one to perform strain engineering within the InGaN-based MQW. Second, owing to significantly different adatom mobilities of Al and In, it could be easier to achieve smoother layers and more abrupt interfaces for AlInN, especially at low growth temperatures, similar to what is observed in AlInAs.[33] Third, at the same lattice constant, and hence the same strain state, AlInN has a larger bandgap than AlGaN. Thus, AlInN ILs placed on top of InGaN QWs (i.e., close to the p-type layer of the device) could potentially suppress any electron leakage more efficiently.[34] Furthermore, the low growth temperature of AlInN (~700–800 °C) is close to that of the InGaN QW, which potentially benefits the epitaxy of the high Al-content alloy and also suppresses In out-diffusion in InGaN-based nanostructure. Previous reports have proposed and demonstrated AlInN layers in optoelectronic devices,[34–39] electronic devices,[39,40] and thermoelectricity.[41–43] However, employing AlInN as an IL into InGaN/GaN MQW for visible emitters has not yet been reported.

In this letter, integration of an AlInN barrier layer, or interlayer (IL), in an InGaN-based MQW structure with

[a)]Authors to whom correspondence should be addressed: wes212@lehigh.edu and tansu@lehigh.edu

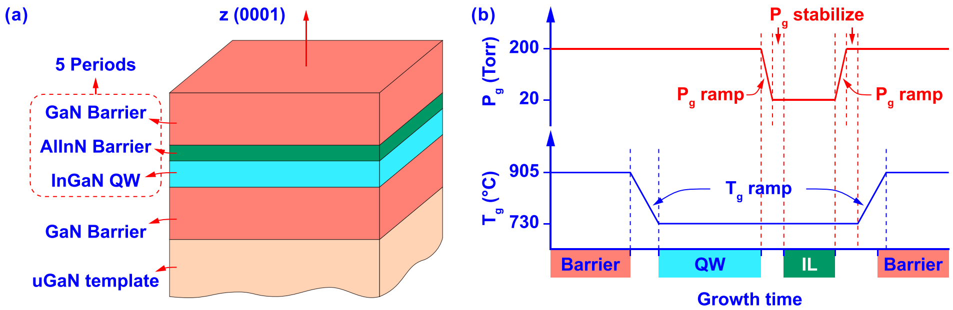

FIG. 1. (a) Schematic illustration of the InGaN-based multiple quantum well (MQW) structure with an AlInN barrier layer or interlayer. (b) Profile of growth temperature (T_g) and pressure (P_g) as function of time for one period of the MQW growth. Note the growth time of each region is not to the same scale in this plot.

significantly enhanced green emission is demonstrated. A growth procedure is developed to accommodate the reduction in growth pressure that is necessary for the AlInN layer without compromising the InGaN QW. X-ray diffraction (XRD) omega-2theta (ω-2θ) scans suggests that embedding an AlInN tensile IL helps to achieve consistently abrupt heterojunctions, similar to InGaN-based MQWs with AlGaN ILs. Room temperature photoluminescence (PL) measurements of the AlInN ILs MQW shows similar performance to MQWs with AlGaN ILs, and ~4–7 times larger radiative efficiency at green wavelengths than conventional InGaN/GaN MQWs.

The InGaN-based MQW structure with an AlInN IL is grown by using metalorganic chemical vapor deposition (MOCVD) in a vertical-flow, Veeco P-75 reactor. Ammonia (NH_3) is used as group-V precursor for all layers, and triethylgallium (TEGa), trimethylindium (TMIn), and trimethylaluminium (TMAl) are used as group-III precursors for the MQW active region. The epitaxy process is initiated with the growth of an 800 nm thick GaN buffer layer at ~1050 °C on a 3 μm thick unintentionally doped GaN (n ~ $3 \times 10^{16}\,cm^{-3}$) on a *c*-plane sapphire substrate, and then followed by the growth of 5 periods of the MQW structure. A single period of the MQW consists of an InGaN QW, a thin AlInN barrier, and thicker GaN barrier as shown in Fig. 1(a). Three MQWs with AlInN IL are fabricated and their structural parameters are listed in Table I (labeled A1, A2, and A3). Two of the AlInN ILs are tensile strained (A1, and A3) while the other (A2) is lattice matched to GaN. For comparison, MQWs with AlGaN tensile strained ILs (samples B1, B2, and B3), and a conventional InGaN/GaN MQW (C1) are grown. The MQWs with AlGaN IL are samples from our previous report.[31]

The growth sequence of the MQW with an AlInN IL is similar to MQWs with AlGaN ILs,[26–31] but with the additional challenge of changing growth pressures. Reported optimized growth pressures (P_g) for AlInN range from ~20 to ~50 Torr,[37–39,41–44] which is significantly lower than that of the InGaN QWs (P_g ~ 200 Torr).[31] This requires a dramatic change of pressure during growth of the MQW, which could potentially cause detrimental turbulences inside the reactor and compromise the quality and performance of the MQW. In this study, the growth pressure of AlInN is set to 20 Torr for optimized material quality,[44] and a "ramp and stabilize" process is employed to achieve stable growth condition for the AlInN. As shown in Fig. 1(b), the P_g is set to 200 Torr for the growth of GaN barrier and InGaN QW, then it is ramped down rapidly in 18 s and stabilized at 20 Torr. Once the P_g is stable the high quality AlInN IL is deposited on top of the InGaN QW layer. Afterwards, the P_g is ramped back in 36 s to 200 Torr and is stabilized for the next period of GaN barrier and InGaN QW. Furthermore, the InGaN QW and AlInN barrier are both grown at T_g = ~730 °C, while the GaN barrier is grown at ~905 °C.

The AlInN IL MQWs are characterized by using XRD ω-2θ scans in the (0002) direction. The upper blue line in Fig. 2 shows the XRD ω-2θ scan of the MQW consisting of ~3.3 nm thick $In_{0.19}Ga_{0.81}N$ QWs, ~1 nm thick $Al_{0.89}In_{0.11}N$ tensile ILs, and ~10 nm thick GaN barriers (sample A1 in Table I). For comparison, the lower orange line in Fig. 2 shows the XRD ω-2θ scan of the conventional InGaN MQW with ~3.3 nm thick $In_{0.19}Ga_{0.81}N$ QWs and ~10 nm thick GaN barriers (sample C1). As shown in Fig. 2, the XRD ω-2θ scan of the MQW with AlInN ILs has significantly sharper high order superlattice (SL) peaks (at ~15°) than that of the conventional MQW, suggesting higher fidelity or more abrupt heterointerfaces. Such phenomenon is similar to MQWs with AlGaN ILs and is attributed to two reasons. First, the AlInN IL caps the InGaN QW and prevents the out-diffusion of In into GaN barriers;[26,27] second, the AlInN IL is tensile strained and compensates the compressive strain within the InGaN QW enabling the consistent nearly pseudomorphic growth of entire 5-period MQW.[31]

TABLE I. InGaN-based MQW samples in PL peak intensity comparison.[a]

Sample ID	In-content of InGaN	InGaN thickness (nm)	Al-content of AlInN	AlInN thickness	Al-content of AlGaN	AlGaN thickness
A1	0.19	3.3	0.89	1 nm	n/a	n/a
A2	0.15	3.3	0.83	1 nm	n/a	n/a
A3	0.19	3.0	0.89	1 nm	n/a	n/a
B1	0.20	3.3	n/a	n/a	0.42	0.4 nm
B2	0.21	3.3	n/a	n/a	0.42	1.0 nm
B3	0.21	3.3	n/a	n/a	0.42	1.7 nm
C1	0.19	3.3	n/a	n/a	n/a	n/a

[a]All MQW samples have ~10 nm thick GaN barriers and consist of 5 periods.

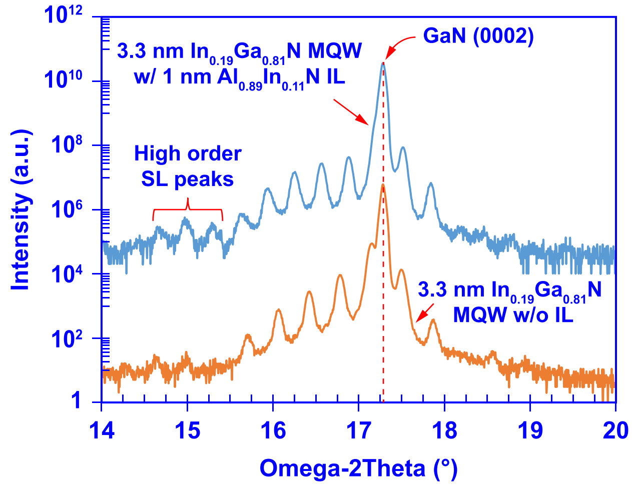

FIG. 2. XRD ω-2θ scan of a 5-period InGaN MQW with ~3.3 nm thick $In_{0.19}Ga_{0.81}N$ QWs, ~1 nm thick $Al_{0.89}In_{0.11}N$ interlayers, and ~10 nm thick GaN barriers, and of a conventional 5-period InGaN MQW with ~3.3 nm thick $In_{0.19}Ga_{0.81}N$ QWs and ~10 nm thick GaN barriers. The AlInN IL MQW data is offset by 10^4 in the y-axis to easily compare data. The higher order superlattice (SL) peaks (at ~15°) are more visible for the AlInN IL MQW.

Photoluminescence (PL) of the samples are measured at T = 300 K by using a 405-nm laser with ~400 μm beam diameter and at ~24 W/cm^2 power density. The as-measured spectra are processed by fast Fourier transform (FFT) to remove resonant fringes caused by the AlInGaN layers on sapphire. Figure 3(a) shows the comparison of PL spectra between the MQW with AlInN ILs and conventional MQW. The AlInN IL MQW (A1) produces higher but broader PL spectrum than the conventional MQW (C1). The peak PL intensity of the MQW with AlInN IL is ~5 times larger than that of the conventional MQW. Such great enhancement in green emission is in consistent with the improved MQW heterointerfaces revealed by XRD. Furthermore, it has been shown theoretically that employing a large bandgap AlInN barrier can also improve the quantum confinement within the QW resulting in stronger optical transitions and higher emission efficiency.[29]

The PL spectrum of the AlInN IL MQW (A1) has a broader full width at half maximum (FWHM) of ~44 nm compared to the conventional MQW as shown in Fig. 3(a). The broadening of the PL spectrum in MQW with AlInN ILs could be attributed to the inhomogeneous growth of the MQW caused by the pressure changes and unstable growth. Although P_g is stabilized before layer growth, small turbulence can exist near the reaction surface after growth restarts. Thus, the MQW thickness can be locally less uniform leading to the broadening. Therefore, it is possible the performance of the MQW with an AlInN IL can be further enhanced if growth with more consistent pressures is applied. On the other hand, even with the current conditions, there is remarkable enhancement in green emission illustrating the AlInN IL is beneficial for potential LED applications.

Figure 3(b) shows the relative radiative efficiencies as function of excitation power density of the same samples shown in Fig. 3(a). The relative radiative efficiency is calculated as the ratio of the integrated PL intensity over the corresponding excitation power. As shown in Fig. 3(b), the relative radiative efficiency of the AlInN IL MQW (A1) exhibits a dramatic enhancement over that of the conventional InGaN MQW (C1). Specifically, 4–7 times improvement is observed over a range of excitation power density. Furthermore, the relative radiative efficiency of AlInN IL MQW peaks at much lower power density. These lower power density and higher peak efficiency are consistent with a decrease in defect or Shockley-Read-Hall recombination. The AlInN IL MQW is behaving similar to AlGaN IL MQWs, where the AlInN behaves as a "cap" layer and the annealing cycle during the GaN barrier growth significantly enhances radiative efficiency of the InGaN QW.[27]

To show how performance varies with emission wavelength, a comparison of PL peak intensity at a pump excitation intensity of ~24 W/cm^2 is carried out among 7 different InGaN-based MQWs. Figure 4 shows the PL peak intensities measured from those 7 different MQWs as function of peak emission wavelength. Note that the PL spectra are mapped at 15 different spots on each MQW sample and the samples are grown on a one-sixth of a 2-in. diameter wafer. The lowest intensity in those 15 measurements is excluded from this plot to avoid the occasional "dead spot" on the sample.

As shown in Fig. 4, A1 has the longest average emission wavelength at ~530 nm with lowest average intensity (~1.8 a.u.) among the MQWs with an AlInN IL. By reducing the QW thickness to 3 nm, the average emission wavelength of A3 blue shifts to ~510 nm with highest average intensity (~2.9 a.u.). As indicated by the dotted red arrow in Fig. 4, the average peak intensity of the MQWs with either the AlInN or AlGaN IL drops as the emission wavelength red shifts which is typical for InGaN-based MQWs. The spread in the peak intensity within a wafer could be due to a number of factors, including growth non-uniformities and resonant PL pumping caused by thickness variations in the underlying GaN. However, the AlInN IL MQWs achieve 4–5 times

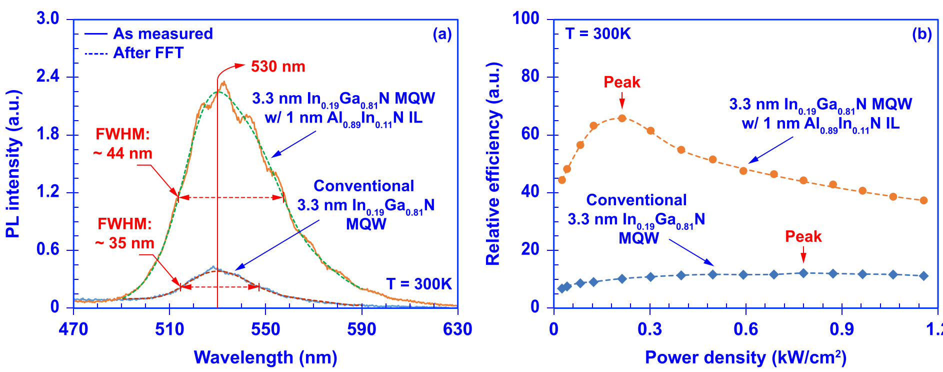

FIG. 3. (a) PL spectra (T = 300 K) of the MQW with 3.3 nm thick $In_{0.19}Ga_{0.81}N$ QWs and 1 nm thick $Al_{0.89}In_{0.11}N$ ILs, and the conventional MQW with 3.3 nm thick $In_{0.19}Ga_{0.81}N$ QWs. (b) The relative radiative efficiency as function of the excitation power density of the same AlInN IL MQW and conventional MQW.

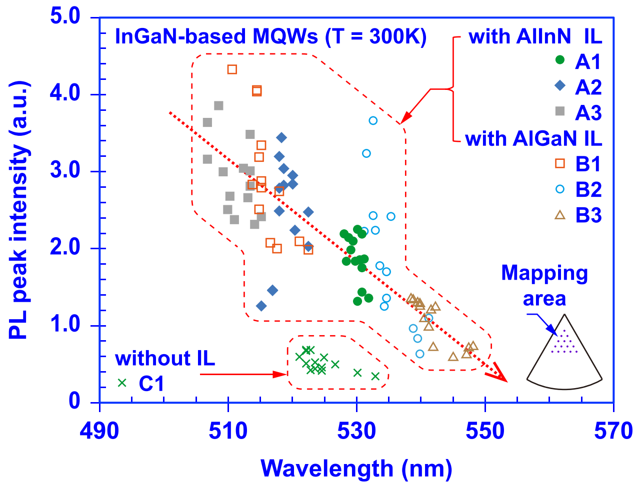

FIG. 4. PL peak intensity comparison (T = 300 K) of the 7 different InGaN-based MQW samples. For each MQW sample, PL spectra are mapped at 15 different spots with their peak intensities plotted as function of peak wavelength.

enhancement on peak PL intensity over the conventional MQW (C1) within the green spectral regime from 520 to 530 nm. Such great improvement shows the advantage of using AlInN ILs in InGaN-based MQWs for high performance green emission. Additionally, Fig. 4 shows that the AlInN IL MQWs have enhancements that are similar to AlGaN IL MQWs. Although the AlGaN IL MQW is a more researched approach for high efficiency long wavelength emitters,[26–31] this data shows AlInN IL could still provide remarkable advantages owing to its high Al-content for better capping and smoothing effects for abrupt interface and add flexibility of tuning strain from tensile to compressive by changing In-content. Furthermore, the AlInN IL on top of InGaN QW serves as larger bandgap barrier, which, in principle, can suppress any electron leakage and enhance current injection efficiency.[34] The benefits of strain engineering and carrier leakage suppression using AlInN ILs require further investigation.

It should be noted that the absolute values of improvement found here could be different for others depending on the maturity of the growth process for the InGaN-based MQWs. The performance of the conventional MQWs shown above is typical for the employed recipe and reactor, and the comparisons show in this letter provide a reasonable metric for improvement. However, it has been shown that AlGaN ILs provide marked improvement over conventional MQWs emitting in the red-green[25–30] and given that the AlInN IL MQWs shown here have similar performance to AlGaN IL MQWs is an indication that they too could provide large improvements for long wavelength InGaN MQWs.

In conclusion, AlInN ILs were integrated into InGaN-based MQWs by MOCVD resulting in enhanced green emission compared to conventional InGaN MQWs. XRD ω-2θ scans of the AlInN IL MQWs exhibited improved fidelity for higher order peaks, suggesting consistently abrupt heterointerfaces due to the AlInN IL. PL measurements on the MQW with 3.3 nm thick $In_{0.19}Ga_{0.81}N$ QWs and 1 nm thick $Al_{0.89}In_{0.11}N$ tensile strained ILs shows 4–7 times higher efficiencies than the conventional InGaN-based MQWs emitting in the green spectral regime. Furthermore, comparison of PL peak intensity of various InGaN-based MQW samples indicates an advantage for the AlInN IL MQWs across a broad portion of the green spectral regime.

The authors would like to acknowledge funding support from U.S. National Science Foundation (Awards Nos. ECCS 1408051 and DMR 1505122) and Daniel E. '39 and Patricia M. Smith Endowed Chair Professorship Fund.

[1]S. Nakamura, T. Mukai, and M. Senoh, Appl. Phys. Lett. **64**, 1687–1689 (1994).
[2]M. R. Krames, O. B. Shchekin, R. Mueller-Mach, G. O. Mueller, L. Zhou, G. Harbers, and M. G. Craford, J. Disp. Technol. **3**, 160–175 (2007).
[3]Y. K. Ee, J. M. Biser, W. Cao, H. M. Chan, R. P. Vinci, and N. Tansu, IEEE J. Sel. Top. Quantum Electron. **15**, 1066–1072 (2009).
[4]N. Tansu, H. P. Zhao, G. Y. Liu, X. H. Li, J. Zhang, H. Tong, and Y. K. Ee, IEEE Photonics J. **2**, 241–248 (2010).
[5]J. J. Wierer, J. Y. Tsao, and D. S. Sizov, Laser Photonics Rev. **7**, 963–993 (2013).
[6]J. Y. Tsao, M. H. Crawford, M. E. Coltrin, A. J. Fischer, D. D. Koleske, G. S. Subramania, G. T. Wang, J. J. Wierer, and R. F. Karlicek, Adv. Opt. Mater. **2**, 809–836 (2014).
[7]M. H. Crawford, IEEE J. Sel. Top. Quantum Electron. **15**, 1028–1040 (2009).
[8]J. M. Phillips, M. E. Coltrin, M. H. Crawford, A. J. Fischer, M. R. Krames, R. Mueller-Mach, G. O. Mueller, Y. Ohno, L. Rohwer, J. A. Simmons *et al.*, Laser Photonics Rev. **1**, 307–333 (2007).
[9]J. J. Wierer and J. Y. Tsao, Phys. Status Solidi A **212**, 980–985 (2015).
[10]R. Singh, D. Doppalapudi, T. D. Moustakas, and L. T. Romano, Appl. Phys. Lett. **70**, 1089 (1997).
[11]N. A. El-Masry, E. L. Piner, S. X. Liu, and S. M. Bedair, Appl. Phys. Lett. **72**, 40 (1998).
[12]X. H. Wu, C. R. Elsass, A. Abare, M. Mack, S. Keller, P. M. Petroff, S. P. DenBaars, J. S. Speck, and S. J. Rosneret, Appl. Phys. Lett. **72**, 692 (1998).
[13]H. K. Cho, J. Y. Lee, G. M. Yang, and C. S. Kim, Appl. Phys. Lett. **79**, 215 (2001).
[14]D. D. Koleske, S. R. Lee, G. Thaler, M. H. Crawford, M. E. Coltrin, and K. C. Cross, Appl. Phys. Lett. **97**, 071901 (2010).
[15]D. D. Koleske, A. E. Wickenden, R. L. Henry, and M. E. Twigg, J. Cryst. Growth **242**, 55–69 (2002).
[16]A. M. Armstrong, M. H. Crawford, and D. D. Koleske, Appl. Phys. Express **7**, 032101 (2014).
[17]U. T. Schwarz, H. Braun, K. Kojima, Y. Kawakami, S. Nagahama, and T. Mukai, Appl. Phys. Lett. **91**, 123503 (2007).
[18]H. P. Zhao, G. S. Huang, G. Y. Liu, X. H. Li, J. D. Poplawsky, S. T. Penn, V. Dierolf, and N. Tansu, Appl. Phys. Lett. **95**, 061104 (2009).
[19]H. P. Zhao, G. Y. Liu, J. Zhang, J. D. Poplawsky, V. Dierolf, and N. Tansu, Opt. Express **19**, A991–A1007 (2011).
[20]H. P. Zhao, G. Y. Liu, and N. Tansu, Appl. Phys. Lett. **97**, 131114 (2010).
[21]C. K. Tan, D. Borovac, W. Sun, and N. Tansu, Sci. Rep. **6**, 19271 (2016).
[22]R. M. Farrell, E. C. Young, F. Wu, S. P. DenBaars, and J. S. Speck, Semicond. Sci. Technol. **27**, 024001 (2012).
[23]Y. Zhao, H. Fu, G. T. Wang, and S. Nakamura, Adv. Opt. Photonics **10**, 246–308 (2018).
[24]J. Zhang and N. Tansu, J. Appl. Phys. **110**, 113110 (2011).
[25]D. M. Van Den Broeck, D. Bharrat, A. M. Hosalli, N. A. El-Masry, and S. M. Bedair, Appl. Phys. Lett. **105**, 031107 (2014).
[26]S. Saito, R. Hashimoto, J. Hwang, and S. Nunoue, Appl. Phys. Express **6**, 111004 (2013).
[27]D. D. Koleske, A. J. Fischer, B. N. Bryant, P. G. Kotula, and J. J. Wierer, J. Cryst. Growth **415**, 57–64 (2015).
[28]J. Hwang, R. Hashimoto, S. Saito, and S. Nunoue, Appl. Phys. Express **7**, 071003 (2014).
[29]H. P. Zhao, R. A. Arif, Y. K. Ee, and N. Tansu, IEEE J. Quantum Electron. **45**, 66–78 (2009).
[30]K. Lekhal, B. Damilano, H. T. Ngo, D. Rosales, P. De Mierry, S. Hussain, P. Vennéguès, and B. Gil, Appl. Phys. Lett. **106**, 142101 (2015).
[31]S. A. A. Muyeed, W. Sun, X. Wei, R. Song, D. D. Koleske, N. Tansu, and J. J. Wierer, AIP Adv. **7**, 105312 (2017).
[32]I. Vurgaftman and J. R. Meyer, in *Nitride Semiconductor Devices*, edited by J. Piprek (Wiley, Berlin, 2007), pp. 13–37.

[33]J. P. Praseuth, L. Goldstein, P. Hénoc, J. Primot, and G. Danan, J. Appl. Phys. **61**, 215 (1987).
[34]G. Y. Liu, J. Zhang, C. K. Tan, and N. Tansu, IEEE Photonics J. **5**, 2201011 (2013).
[35]H. J. Kim, S. Choi, S. Kim, J. Ryou, P. D. Yoder, R. D. Dupuis, A. M. Fischer, K. Sun, and F. A. Ponce, Appl. Phys. Lett. **96**, 101102 (2010).
[36]C. K. Tan, W. Sun, D. Borovac, and N. Tansu, Sci. Rep. **6**, 22983 (2016).
[37]J. F. Carlin, J. Dorsaz, E. Feltin, R. Butté, N. Grandjean, M. Ilegems, and M. Laügt, Appl. Phys. Lett. **86**, 031107 (2005).
[38]S. Nicolay, J. F. Carlin, E. Feltin, R. Butté, M. Mosca, N. Grandjean, M. Ilegems, M. Tchernycheva, L. Nevou, and F. H. Julien, Appl. Phys. Lett. **87**, 111106 (2005).
[39]R. Butte, J. F. Carlin, E. Feltin, M. Gonschorek, S. Nicolay, G. Christmann, D. Simeonov, A. Castiglia, J. Dorsaz, H. J. Buehlmann *et al.*, J. Phys. D: Appl. Phys. **40**, 6328–6344 (2007).
[40]M. Gonschorek, J. F. Carlin, E. Feltin, M. A. Py, and N. Grandjean, Appl. Phys. Lett. **89**, 062106 (2006).
[41]H. Tong, J. Zhang, G. Y. Liu, J. Herbsommer, G. S. Huang, and N. Tansu, Appl. Phys. Lett. **97**, 112105 (2010).
[42]J. Zhang, H. Tong, G. Y. Liu, J. A. Herbsommer, G. S. Huang, and N. Tansu, J. Appl. Phys. **109**, 053706 (2011).
[43]J. Zhang, S. Kutlu, G. Y. Liu, and N. Tansu, J. Appl. Phys. **110**, 043710 (2011).
[44]G. Y. Liu, J. Zhang, X. H. Li, G. S. Huang, T. Paskova, K. R. Evans, H. P. Zhao, and N. Tansu, J. Cryst. Growth **340**, 66–73 (2012).